Available online at www.sciencedirect.com
ScienceDirect
Ceramics International 38 (2012) 389–394
CERAMICS INTERNATIONAL
www.elsevier.com/locate/ceramint

A novel process to synthesize high-k 'Y5V' nanopowder and ceramics

Xinxing Zhan, Bin Cui *, Yilin Xing, Rong Ma, Ying Xie, Zhuguo Chang, Fengxing Zhang

Key Laboratory of Synthetic and Natural Functional Molecule Chemistry (Ministry of Education), Shaanxi Key Laboratory of Physico-Inorganic Chemistry, School of Chemistry & Materials Science, Northwest University, Xi'an 710069, PR China

Received 26 April 2011; received in revised form 7 July 2011; accepted 8 July 2011
Available online 19th July 2011

Abstract

The present work proposes a simple one-step sol–gel process for the synthesis of high-k $(Ba_{0.87}Sr_{0.04}Ca_{0.09})(Ti_{0.86}Zr_{0.08}Sn_{0.06})O_3$ (BSCTZS) powders and ceramics. Characterization using TG-DTG, XRD, SEM and TEM methods reveals that the powders are of nanometer scale and exhibit a cubic perovskite structure. After sintering, cubic $BaTiO_3$ structure ceramics were obtained. Compared to the traditional method of preparation, the powders and ceramics prepared by the one-step sol–gel process exhibit a high dielectric constant due to narrow grain size distribution, controlled morphology, and high purity. Doped niobium decreases the grain size of BSCTZS ceramics and lowers the Curie temperature. At a Nb concentration of 0.38 mol%, BSCTZS ceramics meet the EIA Y5V specifications and the room temperature (25 °C) permittivity is greater than 16,000. The BSCTZS nanopowders prepared through the process with uniformity component will increase the volumetric efficiency of multi-layer ceramic capacitors by decreasing the dielectric layer thickness. Most importantly, this new approach greatly simplifies the preparation processes.

Keywords: A. Sol–gel process; C. Dielectric properties; Barium titanate; Nb-doped; Y5V

1. Introduction

Research on temperature stable, $BaTiO_3$-based dielectrics is undergoing rapid development owing to the desirable qualities of these compounds, which exhibit a high dielectric constant, high tunability, and excellent ferroelectric and piezoelectric properties [1]. Commonly used in multi-layer ceramic capacitors (MLCC), the temperature coefficient of capacitance (TCC) of this material must conform to the EIA Y5V specification ($-82\% \leq (\varepsilon - \varepsilon_{RT})/\varepsilon_{RT} \leq +22\%$ in a temperature range from −30 to 85 °C). The substitution of Zr^{4+}, Sn^{4+} at the Ti^{4+} site and Sr^{2+}, Ca^{2+} at the Ba^{2+} site results in a strong broadening of the Curie temperature peak and further ''relaxor''-type ''Y5V'' behavior, with room temperature permittivity (ε_r) increasing to ∼10,000 for modified ceramics with Curie temperature (T_C) near room temperature [2–4]. Niobium is a typical donor element and doping with niobium can inhibit the $BaTiO_3$-based ceramic grain growth, and improve the dielectric properties of $BaTiO_3$ ceramics [5–7]. Moreover, a small variation of the dielectric constant with temperature can be achieved by introducing a small amount of niobium to the microstructure of $BaTiO_3$. It has also been shown that the addition of niobium at low concentrations can decrease dielectric loss through a charge compensation mechanism resulting from electron mobility, which causes an important reduction of the titanium valence (Ti^{4+} to Ti^{3+}) [8].

MLCC require superfine powders with nanoscale particle size because they contain multiple dielectric layers, each of which must be as thin as possible. Typically, a traditional solid-state method is used to prepare Y5V-compliant ceramics, but this traditional method often produces non-homogeneously doped powders, which seriously affect the stability of product performance [9]. Powders produced using the solid-state method also consist of large particles. Nano-sized $BaTiO_3$-based powder is usually prepared through wet chemical routes such as the precipitation method, the hydrothermal method, and the sol–gel process [10,11]. Among these wet methods the first two require comparatively complicated technological conditions; both involve washing processes and are hard to control in actual production. The sol–gel method offers clear advantages by permitting a relatively low-temperature process that avoids contamination of the materials. It also yields better stoichiometric control and the possibility of both grain-size and grain-shape control. Alcoholic niobium is a common reagent which is

* Corresponding author. Tel.: +86 29 88302604; fax: +86 29 88302604.
E-mail address: cuibin@nwu.edu.cn (B. Cui).

0272-8842/$36.00.
doi:10.1016/j.ceramint.2011.07.018

added to the mother colloid during the sol–gel process, but the method has been reported on infrequently because of the high cost of alcoholic niobium.

In this paper, we report on a simple one-step sol–gel method to synthesize Nb-doped $(Ba_{0.87}Sr_{0.04}Ca_{0.09})(Ti_{0.86}Zr_{0.08}Sn_{0.06})O_3$ (BSCTZS) nanopowders and ceramics. A water-soluble compound of niobium ($H_3[Nb(O_2)_4]$), rather than expensive alcoholic niobium, was used as a precursor. The one-step sol–gel method to synthesize nano-crystalline powders and ceramics increases the volumetric efficiency of the MLCCs by decreasing the dielectric layer thickness, thus enabling manufacturers to meet the current demand for device miniaturization in the electronics industry.

2. Experimental

2.1. Chemicals and equipment

For this study, we used chemically pure $C_{32}H_{64}O_4Sn$ (99.00%, C.P.) as well as analytically pure, $Ti(OC_4H_9)_4$, $Ba(CH_3COO)_2$, $Sr(NO_3)_2$, $Ca(CH_3COO)_4$, $ZrO(NO_3)_2$, and Nb_2O_5 as reagents. We prepared solutions of $H_3[Nb(O_2)_4]$ following the method of Das and Pramanik [12].

We studied the thermal behavior (DSC-TGA) of the xerogels using an SDT Q600 thermal analyzer (TA Instruments) over a temperature range of 50–1000 °C (at 10 °C/min) within a dynamic air atmosphere. The structure of the BSCTZS powders and ceramics were determined by means of X-ray diffraction (XRD; D8 ADVANCE™, Bruker AXS, Frankfurt, Germany) and the powder microstructures were observed using an H-600 transmission electron microscope (TEM; Hitachi High-Technologies Corporation, Japan). We characterized the microstructures of the as-sintered ceramic samples using an S-570 scanning electron microscope (SEM; Hitachi High-Technologies Corporation, Japan). Finally, we measured dielectric properties of the ceramics using an LCR meter (HP 4284A, Hewlett-Packard, U.S.A.), computer controlled at 1 kHz, and temperature controlled between −50 and 150 °C using high and low gimbals (GDW-100E, China).

2.2. Preparation of the BSCTZS powders and ceramics

We synthesized Nb-doped BSCTZS compositions via the sol–gel process. First, we mixed $Ti(OBu)_4$ with glacial acetic acid and absolute ethanol at room temperature; then we dissolved dibutyltin dilaurate in absolute ethanol and added it to the $Ti(OBu)_4$/ethanol solution. Separately, we produced an aqueous solution of $Ba(CH_3COO)_2$, $Ca(CH_3COO)_2$, $Sr(NO_3)_2$, $ZrO(NO_3)_2$ and $H_3[Nb(O_2)_4]$, added it to the former mixture (pH = 4), and stirred vigorously for 30 min to form a homogeneous mixture. Gelling occurred at 40–50 °C; dry gels were obtained by heating at 70 °C for approximately 24 h. We prepared the BSCTZS nanopowders by calcining the dry gels at 900 °C for 2 h. The powders were pressed into 12 mm diameter discs with a uniaxial force of approximately 6 MPa, and subsequently sintered at 1350 °C for 2 h. Finally, we polished the sintered discs and applied silver paste to both sides of each disc to permit dielectric measurements.

3. Results and discussions

3.1. Thermal analysis and XRD patterns of BSCTZS xerogels

Fig. 1 shows the Thermogravimetric and differential thermogravimetric analysis curve (TG-DTG) for BSCTZS xerogels. To aid in interpreting the TG-DTG analysis for the xerogels at different heat-treatment temperatures, we also present the XRD patterns of the xerogels (Fig. 2). In Fig. 1, the decomposition process (along the TG curve) is divided into two steps. The first step, which occurs between approximately 50 and 650 °C, can be attributed to the complete oxidation and combustion of the nitrate, oxyethyl, acetoxy, butoxy groups, and dibutyltin dilaurate, corresponding to a relatively intense differential peak at 330.3 °C. The $BaCO_3$, $CaCO_3$, $SrZrO_3$ and TiO_2 phases start to appear at this differential peak (Fig. 2). The temperature at which the cubic $SrZrO_3$ perovskite phase begins is low (600 °C), and this facilitates the formation of the $BaTiO_3$-based solid solution. The second step of the mass loss occurs from approximately 650 °C to 760 °C and can be attributed to the formation of the $BaTiO_3$-based solid solution, which corresponds to the differential peak of 738 °C in the DTG curve. When the calcining temperature is greater than 760 °C, the weight of BSCTZS xerogels no longer decreases and production of a large amount of BSCTZS begins. XRD

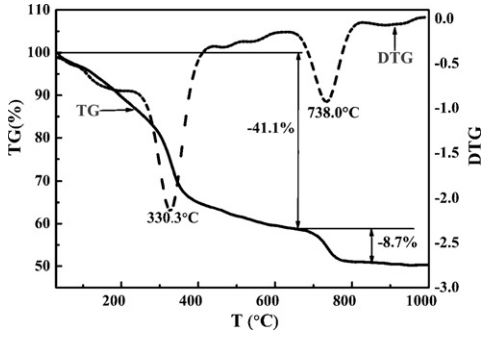

Fig. 1. Thermogravimetric (TG) and differential thermogravimetric (DTG) curves of BSCTZS xerogel.

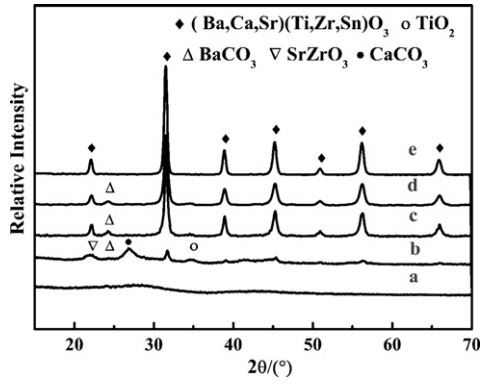

Fig. 2. X-ray diffraction (XRD) patterns for BSCTZS xerogels calcined at different temperatures: (a) 500 °C; (b) 600 °C; (c) 700 °C; (d) 800 °C; (e) 900 °C.

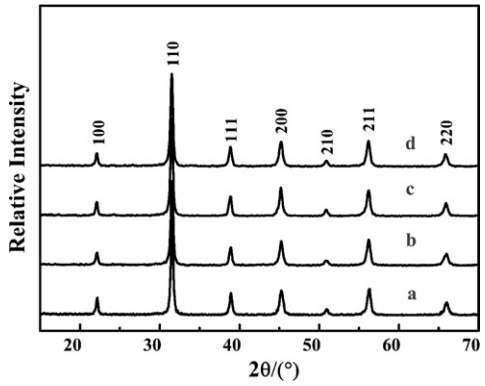

Fig. 3. X-ray diffraction (XRD) patterns for BSCTZS powders with various Nb concentrations after calcining at 900 °C for 2 h: (a) Nb = 0; (b) Nb = 0.23 mol%; (c) Nb = 0.38 mol%; (d) Nb = 0.77 mol%.

confirms that the calcining powders consist mainly of the cubic $BaTiO_3$ structure (JCPDS No. 31-0174) with a small amount of $BaCO_3$ (JCPDS No. 41-0373). As the temperature rises to 900 °C, the calcining powders consist mainly of the cubic perovskite structure without impurities. Thus, the selected calcining temperature of xerogels is 900 °C for a period of 2 h.

3.2. Effect of Nb concentration on phases and morphology of BSCTZS powders

Figs. 3 and 4 show the XRD patterns and TEM images, respectively, of BSCTZS powders calcined at 900 °C for 2 h with different Nb concentrations. Fig. 3 shows that the calcining powders consist mainly of the cubic perovskite structure. Additionally, using the Scherrer formula, and based on the half-width of (1 1 0) reflection of the observed X-ray data, the particle size of BSCTZS powders with different Nb concentrations (0, 0.23, 0.38, and 0.77 mol%) is estimated to range from 20 to 30 nm. No other phases were detected in the XRD patterns of the powders doped with Nb (e.g., crystals related to Nb). Possibly, this is because the concentration of the dopant is below XRD detection limits or because the formation of amorphous compounds cannot be detected. Another possibility is that other phases do not form. The TEM images show that once the powders

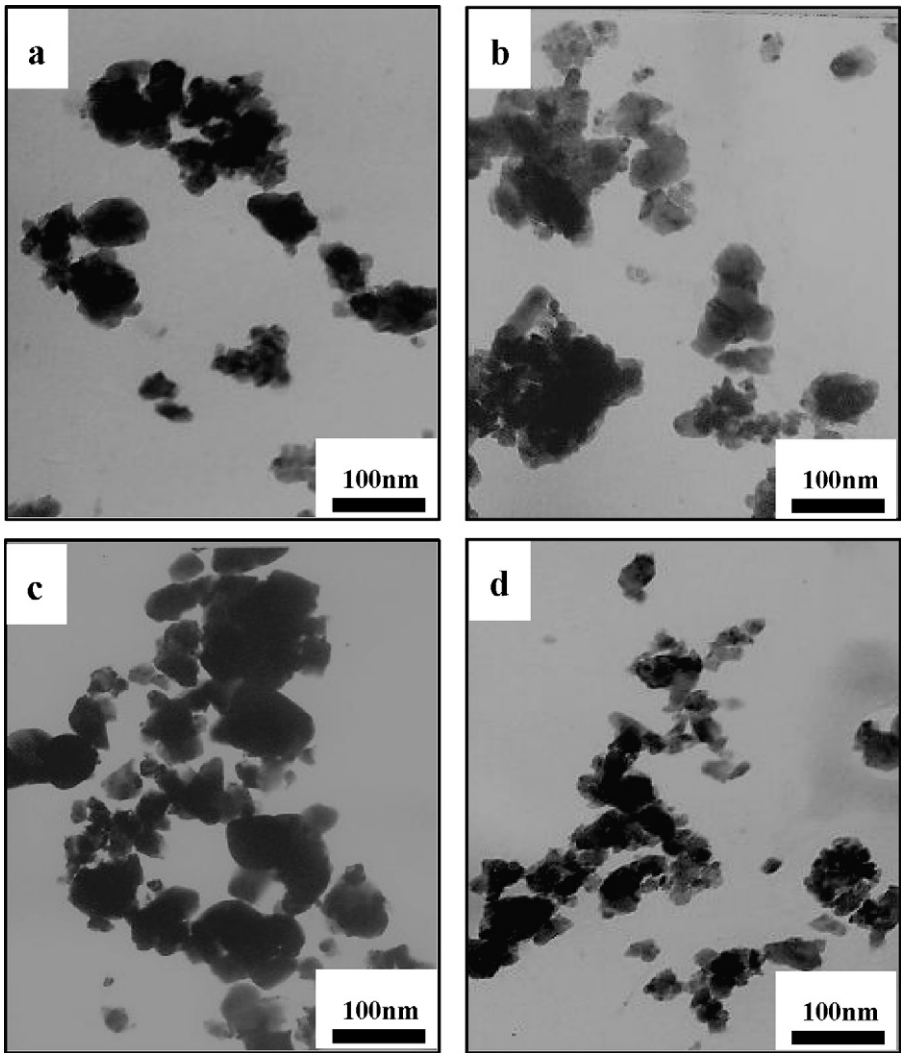

Fig. 4. TEM micrographs of BSCTZS powders with various Nb concentrations after calcining at 900 °C for 2 h: (a) Nb = 0; (b) Nb = 0.23 mol%; (c) Nb = 0.38 mol%; (d) Nb = 0.77 mol%.

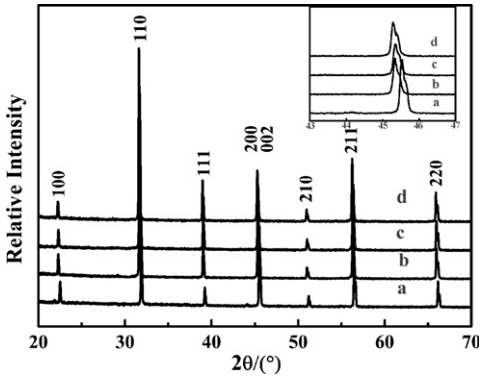

Fig. 5. X-ray diffraction (XRD) patterns for BSCTZS ceramics after calcining at 900 °C for 2 h and sintering at 1350 °C for 2 h: (a) Nb = 0; (b) Nb = 0.23 mol%; (c) Nb = 0.38 mol%; (d) Nb = 0.77 mol%.

are dispersed in the ethanol solvent, some of the powder grains form a chain network with soft agglomeration. From Figs. 3 and 4, we can conclude that Nb has little effect on the phases and morphology of BSCTZS powders. The XRD and TEM analyses confirm that BSCTZS nanopowders are synthesized successfully.

3.3. Effect of Nb concentration on phases and morphology of BSCTZS ceramics

Fig. 5 shows the XRD pattern of BSCTZS ceramics (calcined at 900 °C for 2 h, sintered at 1350 °C for 2 h) with different Nb concentrations (0.23–0.77 mol%). The SEM micrographs of the natural surface of ceramics are shown in Fig. 6. The diffraction peaks of (0 0 2) and (2 0 0) shift to a lower angle as Nb content increases, indicating that BSCTZS ceramic grain size decreases with increasing Nb concentration; this is consistent with the SEM results (Fig. 6). There are two reasons for this phenomenon: (a) the increasing degree of

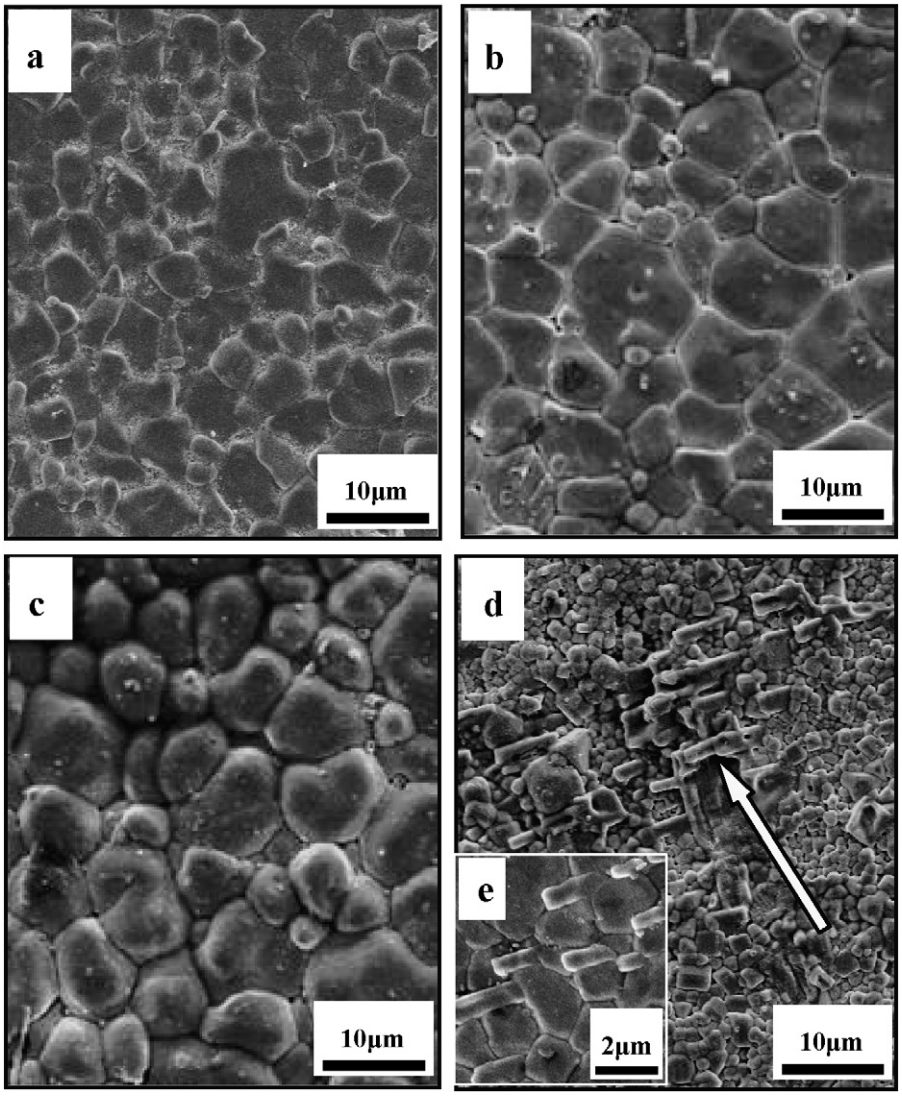

Fig. 6. SEM micrographs of BSCTZS ceramics with various Nb concentrations produced by calcining at 900 °C for 2 h followed by sintering at 1350 °C for 2 h: (a) Nb = 0; (b) Nb = 0.23 mol%; (c) Nb = 0.38 mol%; (d) Nb = 0.77 mol%.

substitution of Ti^{4+} by Nb^{5+} in the perovskite lattice and segregation of the titanium ions from $BaTiO_3$ particles lead to a higher nucleation rate than growth rate and (b) the increased mobility of BSCTZS grain boundaries during sintering, which results from different charge compensations [13].

The sample doped with a Nb concentration higher than 0.38 mol% shows the development of a second phase with the appearance of elongated needles (as indicated by the arrow in Fig. 6(d)); this is consistent with results reported in the literature [14,15]. Due to an extraordinary jump in barium vacancies, the composition of the secondary phase corresponds to nonstoichiometric compounds similar to $Ba_6Ti_{14}Nb_2O_{39}$ and $Ba_6Ti_{17}O_{40}$ [12]. However, this composition change was not evident in XRD patterns, perhaps because the concentration of the dopant was below the limits for XRD.

3.4. Effect of Nb concentration on dielectric properties of BSCTZS ceramics

The permittivity–temperature curves of the Nb-doped BCSTZS-based ceramics are shown in Fig. 7 and the main properties of BSCTZS ceramics are provided in Table 1. The T_C of the Nb-doped BSCTZS ceramics indicates that Nb can lower the T_C. The polarization of the Nb^{5+} ion may be stronger than Ti^{4+}, resulting in the decrease of the ionic bond between Nb^{5+} and O^{2-} and lattice energy. When Ti^{4+} is replaced by Nb^{5+}, with a weak combination between Nb–O, the central ion is relatively unstable. In this state, lower thermal motion can break the asymmetric balance, allowing the ceramic to have a lower T_C [16]. The dielectric constant of BSCTZS ceramics first increased and then decreased as the Nb concentration increased. Consistent with the XRD analyses, as more Nb^{5+} is substituted at the Ti-site of the ABO_3 crystal lattice, the defect structure of $Ba^{2+}(Ti_{1-2x}{}^{4+}Nb_x{}^{5+}Ti_x{}^{3+})O_3$ appears in order to maintain a charge balance [17]. When the Ba and O vacancies appear, the internal electric field is augmented resulting in an increasing dielectric constant in the $BaTiO_3$-based ceramics [8]. From the SEM micrographs, we can further conclude that the large grain size of BSCTZS ceramics exacerbates this tendency. As the Nb concentration continues to increase, the development of a second phase (the appearance elongated needles) leads to a decrease in the density of the ceramics accompanied by a decrease in the dielectric constant. At a Nb concentration of 0.38 mol%, BSCTZS ceramics meet the required EIA Y5V specifications and reach a higher room temperature permittivity (over 16,000).

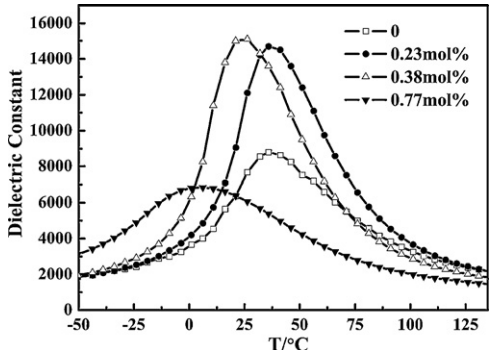

Fig. 7. Temperature dependence of dielectric constant as a function of Nb concentrations for BSCTZS ceramics sintered at 1350 °C for 2 h.

Table 1
Main properties of BSCTZS ceramics at various Nb concentrations.

x_{Nb} (%)	ρ (g/cm^3)	ε_{max}	ε_r (25 °C)	T_C (°C)	TCC (%)		
					−30 °C	T_C	+85 °C
0	5.66	8829	7705	33	−69.8	14.6	−39.8
0.23	5.36	17,417	15,200	35	−83.7	14.5	−65.9
0.38	5.13	16,400	16,200	20	−80.9	1.2	−74.7
0.77	5.17	9750	7175	−5	−34.2	35.8	−64.9

4. Conclusions

Nb-doped high-k $(Ba_{0.87}Sr_{0.04}Ca_{0.09})(Ti_{0.90}Zr_{0.04}Sn_{0.06})O_3$ nanopowder and ceramics were prepared using a one-step sol–gel process. The powders calcined at 900 °C for 2 h had nanoscale particle sizes consisting primarily of a cubic perovskite structure. After sintering, cubic $BaTiO_3$ structure ceramics were obtained. The grain size of the BCSTZS ceramics decreased as the Nb concentration increased. Furthermore, doped niobium lowered the Curie temperature and increased the dielectric constant of the BSCTZS ceramics. At a Nb concentration of 0.38 mol%, the BSCTZS ceramics met the EIA Y5V specifications and the room temperature (25 °C) permittivity was greater than 16,000. Compared with other traditional methods, the powders synthesized by the one-step sol–gel method have a more homogeneous composition and are highly active. Furthermore, the one-step sol–gel method reduces component size and increases the volumetric efficiency of MLCCs by decreasing the dielectric layer thickness. Most importantly, the production process is greatly simplified.

Acknowledgements

This work was supported by the National Natural Science Foundation of China (Grant No. 21071115), the Science Research and Project Program of the Education Committee of Shaanxi Province (No. 09JC01), and the National University Student Innovation Test Plan (No. 201016).

References

[1] D. Hennings, A. Schnell, G. Simon, Diffuse ferroelectric phase transitions in $Ba(Ti_{1-y}Zr_y)O_3$ ceramics, J. Am. Ceram. Soc. 65 (1982) 539–544.
[2] T.A. Jain, K.Z. Fung, J. Chan, Effect of the A/B ratio on the microstructures and electrical properties of $(Ba_{0.95\pm x}Ca_{0.05})(Ti_{0.82}Zr_{0.18})O_3$ for multilayer ceramic capacitors with nickel electrodes, J. Alloys Compd. 468 (2009) 370–374.
[3] S.G. Lee, D.S. Kang, Dielectric properties of ZrO_2-doped $(Ba,Sr,Ca)TiO_3$ ceramics for tunable microwave device applications, Mater. Lett. 57 (2003) 1629–1634.
[4] M. Kumar, A. Garg, R. Kumar, M.C. Bhjatnagar, Structural, dielectric and ferroelectric study of $Ba_{0.9}Sr_{0.1}Zr_xTi_{1-x}O_3$ ceramics prepared by the sol–gel method, Physica B 403 (2008) 1819–1823.

[5] B.D. Stojanovic, M.A. Zaghete, C.R. Foschini, F.O.S. Vieira, J.A. Varela, Structure and properties of donor doped barium titanate prepared by citrate process, Ferroelectrics 270 (2002) 15–20.
[6] W. Li, J.Q. Qi, Y.L. Wang, L.T. Li, Z.L. Gui, Doping behaviors of Nb_2O_5 and Co_2O_3 in temperature stable $BaTiO_3$-based ceramics, Mater. Lett. 57 (2002) 1–5.
[7] S. Wang, S.R. Zhang, X.H. Zhou, B. Li, Z. Chen, Investigation on dielectric properties of $BaTiO_3$ co-doped with Ni and Nb, Mater. Lett. 60 (2006) 909–911.
[8] V.V. Mitić, I. Mitrović, The influence of Nb_2O_5 on $BaTiO_3$ ceramics dielectric properties, J. Eur. Ceram. Soc. 21 (2001) 2693–2696.
[9] B. Cui, P.F. Yu, J. Tian, Z.G. Chang, Preparation and characterization of Co-doped $BaTiO_3$ nanosized powders and ceramics, Mater. Sci. Eng. B 133 (2006) 205–208.
[10] J.F. Chen, Z.G. Shen, F.T. Liu, X.L. Liu, J. Yun, Preparation and properties of barium titanate nanopowder by conventional and high-gravity reactive precipitation methods, Scripta Mater. 49 (2003) 509–514.
[11] M. Boulos, S. Guillemet-Fritsch, F. Mathieu, B. Durand, T. Lebey, V. Bley, Hydrothermal synthesis of nanosized $BaTiO_3$ powders and dielectric properties of corresponding ceramics, Solid State Ionics 176 (2005) 1301–1309.
[12] R.N. Das, P. Pramanik, Chemical synthesis of fine powder of lead magnesium niobate using niobium tartarate complex, Mater. Lett. 46 (2000) 7–14.
[13] X. Xu, G.E. Hilmas, Effects of $Ba_6Ti_{17}O_{40}$ on the dielectric properties of Nb-doped $BaTiO_3$ ceramics, J. Am. Ceram. Soc. 89 (2006) 2496–2501.
[14] E. Brzozowski, M.S. Castro, C.R. Foschini, B. Stojanovic, Secondary phases in Nb-doped $BaTiO_3$ ceramics, Ceram. Int. 28 (2002) 773–777.
[15] B.D. Stojanovic, C.R. Foschini, M.A. Zaghete, F.O.S. Veira, K.A. Peron, M. Cilense, J.A. Varela, Size effect on structure and dielectric properties of Nb-doped barium titanate, J. Mater. Process. Technol. 143–144 (2003) 802–806.
[16] B.R. Li, X.L. Zhang, Inorganic Dielectric Medium, Huazhong University of Science and Technology Press, Wuhan, 1995, p. 12.
[17] J.P. Bonsack, Dielectric properties of barium titanate containing niobium and the effect of additives, Am. Ceram. Soc. Bull. 50 (1971) 488.